# *Supporting Information*

## Carbon Nanotube In-Situ Embedded with NiS Nanocrystals Outperforms to Pt for Dye-Sensitized Solar Cells: Interface Improved Activity

Xiuwen Wang[a], Ying Xie[b], Yanqing Jiao[b], Kai Pan[b, *], Buhe Bateer[b], Jun Wu[a], and Honggang Fu[b, *]

[a] Key Laboratory of Superlight Materials and Surface Technology, Ministry of Education, College of Material Science and Chemical Engineering, Harbin Engineering University, Harbin 150001, China.

[b] Key Laboratory of Functional Inorganic Material Chemistry, Ministry of Education of the People's Republic of China, Heilongjiang University, 150080 Harbin P. R. China. Email: kaipan@hlju.edu.cn, fuhg@vip.sina.com.

## Experimental details

### Materials

Oleylamine (OAm, 70 %), 1-octadecene (ODE, 90 %), oleic acid (OA, 90 %) were purchased from Sigma Aldrich. Nickel chloride ($NiCl_2 \cdot 6H_2O$), sodium oleate, and sulfur powder (S) were obtained from Aladdin Industrial Corporation, China. Ethanol, toluene and n-hexane were obtained from Sinopharm Chemical Reagent Co., Ltd. Multiwalled carbon nanotubes (CNTs, purity ≈ 95 %) were purchased from XFNANO, INC, China. And all of the reagents were used as received.

### Characterizations

The chemical composition of as-synthesized nanomaterial was verified by X-ray diffraction (XRD, Rigaku D/max-IIIB diffractometer with Cu-Kα radiation). Raman spectra were recorded on a Jobin Yvon HR 800 micro-Raman spectrometer at 457.9 nm. X-ray photoelectron spectroscopy (XPS) analysis was carried out on a VG ESCALAB MK II with an Mg Ka (1253.6 eV) achromatic X-ray source. Transmission electron microscopy (TEM) analyses were performed by drop-casting a dilute suspension on carbon-coated copper grid. The corresponding TEM images were obtained with JEM-3010 microscopes operated at 200 kV. Thermogravimetric analyses (TGA) were carried out on TA Q600 at a heating rate of 10 °C/min under an air atmosphere.

J-V curves were measured using an electrochemical analyzer (Zahner Elektrik, Germany) under AM1.5 illumination. Cyclic voltammograms (CVs) analyses were carried out in a three-electrode system in a nitrogen-purged acetonitrile solution, which consist of $LiClO_4$ (0.1 M), LiI (10 mM), and $I_2$ (1 mM) using a BAS100B electrochemical analyzer. The electrochemical impedance spectroscopy (EIS) were performed in a dummy cell with a computer-controlled IM6e impedance measurement unit (Zahner Elektrik, Germany) and carried out by applying sinusoidal perturbations of 10 mV, and the frequency ranges from 10 mHz to 1 MHz. The obtained spectra were fitted with ZsimpWin software in terms of appropriate equivalent circuits. The

Tafel polarization measurements were carried out with BAS100B electrochemical analyzer in a dummy cell.

**Theory calculations**

All calculations were carried out by using the CASTEP package within the density functional theory (DFT) framework.[S1] Perdew-Burke-Ernzerhof functional with a generalized gradient approximation (GGA-PBE) form was adopted to deal with the exchange correlation energies of the systems.[S2] The plane-wave and pseudo-potential techniques were used, and the energy cutoff was 330 eV. To obtain a good numerical sampling of electron densities in Brillouin zone, a (4×4×1) Monkhorst-Pack mesh was applied to the NiS (101) surface and a (2×1×1) one to the NiS/CNTs composite.[S3] Broyden-Fletcher-Goldfarb-Shanno (BFGS) algorithm was used during the geometry optimization, and the optimization procedure was repeated until the force, the stress, and the displacement on each atom were less than 0.01 eV·Å$^{-1}$, 0.02Gpa, 5.0×10$^{-4}$ Å, respectively.[S4] This set of parameters also guarantees that the total energies of the systems are accurate within 5.0×10$^{-6}$ eV. Based on the experimental observations, NiS (101) surface was taken into account. Furthermore, as the diameter of the CNTs is much larger than the NiS particles, a 2D carbon sheet without considering the curvature was introduced as the model substrate for growing NiS nanoparticles. During the calculations, a vacuum layer of 20 Å is used to avoid the fake interactions between periodic images along z axis. To evaluate the bonding strength between $I_3^-$ molecule and the materials, the binding energies ($E_b$) are calculated,

$$E_b = E_{I3-/material} - (E_{I3-} + E_{material})$$

where $E_{I3-}$, $E_{material}$, and $E_{I3-/material}$ represent the total energy of $I_3^-$ free molecule, the energy of material surfaces (NiS and NiS/CNTs), and the energy of $I_3^-$ molecule adsorbed on the material surface, respectively.

## Supplementary results

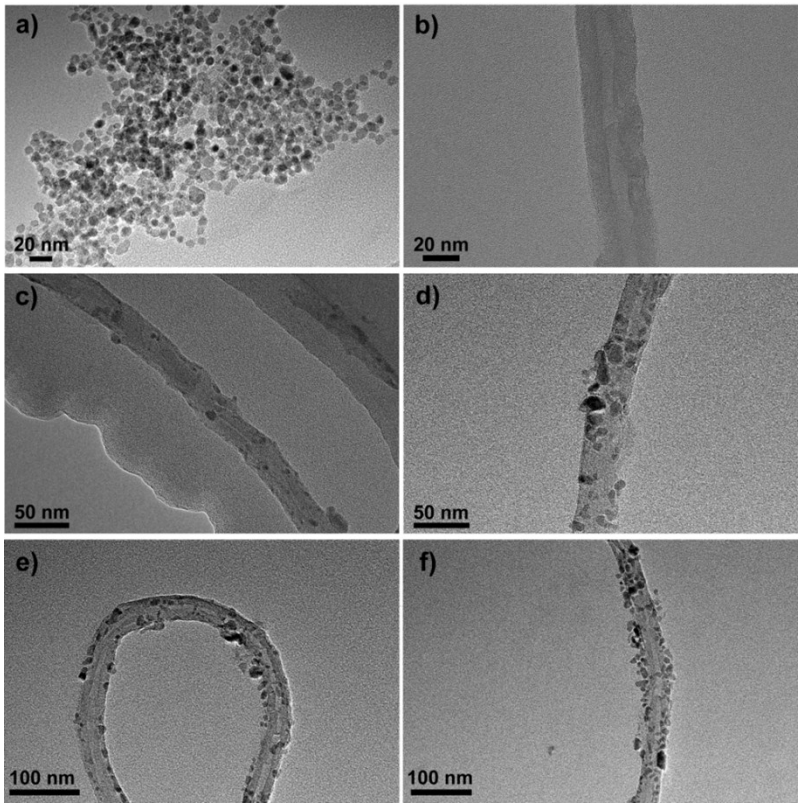


**Fig. S1** TEM images of obtained NiS nanoparticles (a), CNTs (b), NiS-0.75/CNTs (c), NiS-1.00/CNTs (d), NiS-1.50/CNTs (e), and NiS-2.00/CNTs (f), respectively.

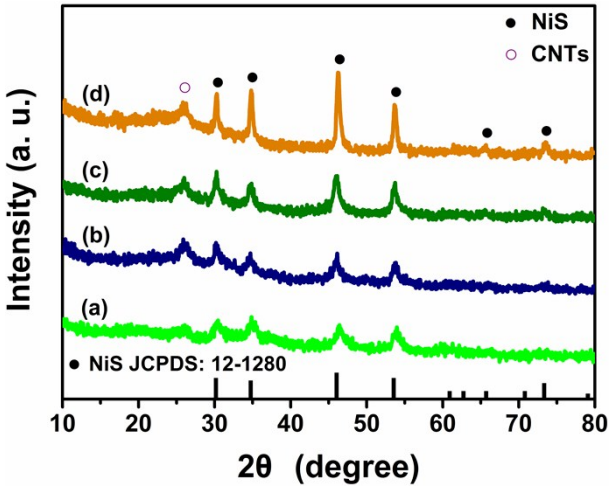


**Fig. S2** XRD patterns of as-prepared NiS-0.75/CNTs (a), NiS-1.00/CNTs (b), NiS-1.50/CNTs (c), and NiS-2.00/CNTs (d), respectively.

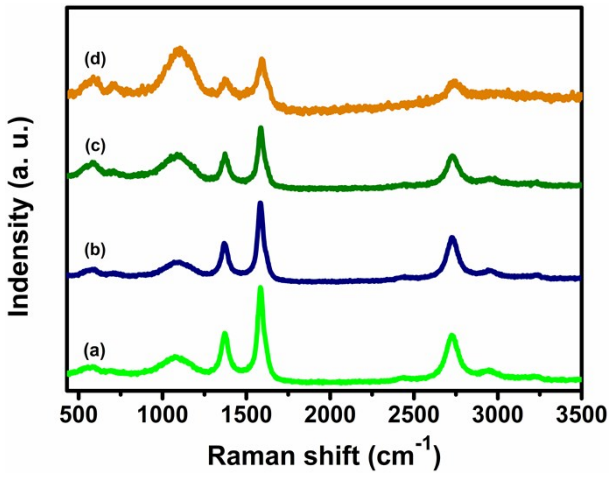


**Fig. S3** Raman spectra of prepared NiS-0.75/CNTs (a), NiS-1.00/CNTs (b), NiS-1.50/CNTs (c), and NiS-2.00/CNTs (d), respectively.

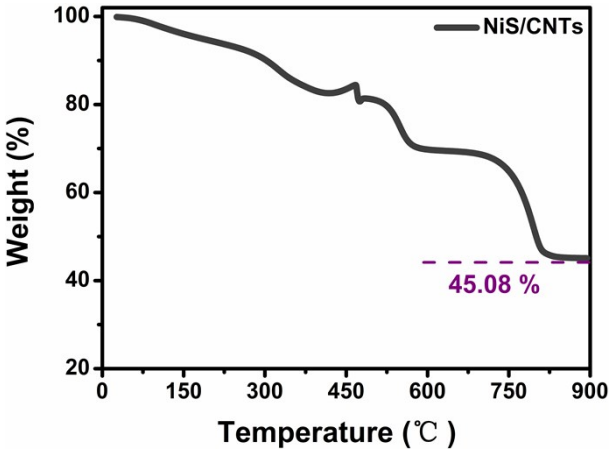


**Fig. S4** TGA curve of NiS/CNTs composite.

**Table S1.** The detailed photovoltaic parameters of the DSSCs using different CEs.

| CEs | $V_{oc}$ (mV) | $J_{sc}$ (mA/cm$^2$) | FF | PCE (%) |
|---|---|---|---|---|
| Pt | 729 | 17.30 | 0.64 | 8.03 |
| NiS-0.75/CNTs | 726 | 19.90 | 0.64 | 9.24 |
| NiS-1.00/CNTs | 728 | 20.79 | 0.65 | 9.84 |
| NiS/CNTs (NiS-1.25/CNTs) | 724 | 22.87 | 0.65 | 10.82 |
| NiS-1.50/CNTs | 729 | 22.11 | 0.64 | 10.27 |
| NiS-2.00/CNTs | 725 | 20.73 | 0.64 | 9.62 |
| NiS | 728 | 16.06 | 0.63 | 7.45 |
| CNTs | 715 | 15.64 | 0.61 | 6.81 |

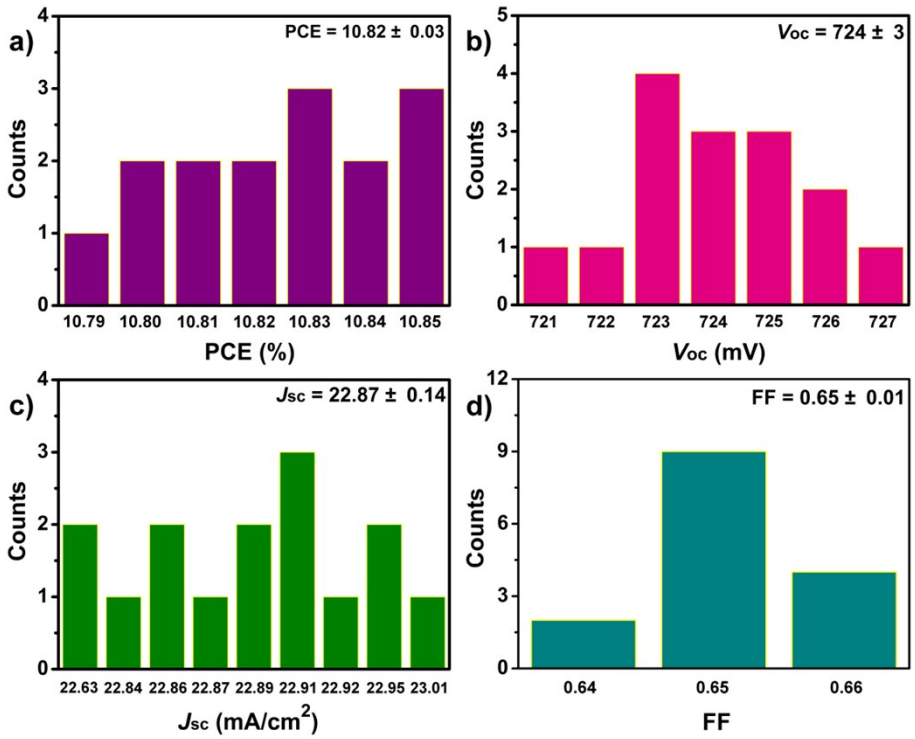


**Fig. S5** Histograms of photovoltaic parameters (PCE (a), $V_{oc}$ (b), $J_{sc}$ (c), and FF (d)) for a series of DSSCs based on NiS/CNTs electrodes, composed of 15 separate devices.

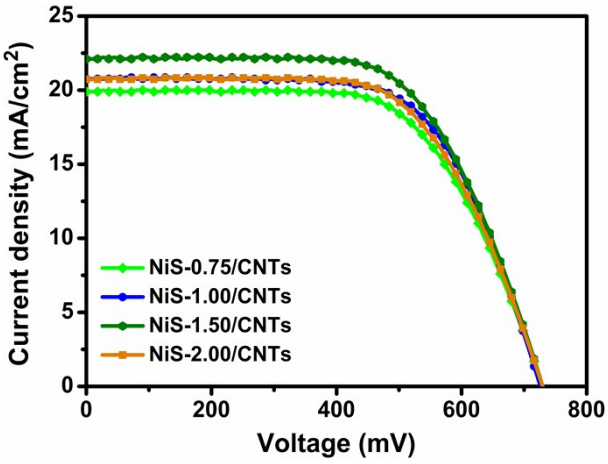


**Fig. S6** J-V curves of DSSCs based on different CEs under AM 1.5.

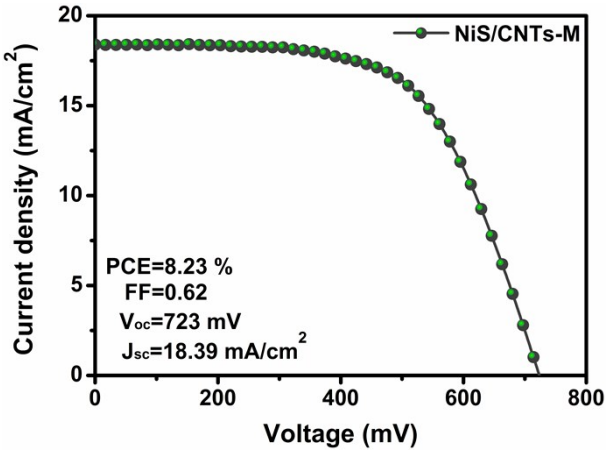


**Fig. S7** J-V curves of DSSCs based on NiS/CNTs-M CE under AM 1.5.

**Table S2**. Photvoltaic parameters of DSSCs based on transition metal sulfide/carbon material composite CEs.

(FTO substrate, $I_3^-/I^-$ redox electrolyte, N719 dye, irradiation intensity: 100 mW $cm^{-2}$)

| CEs | $J_{sc}$ (mA/$cm^2$) | $V_{oc}$ (V) | FF | PCE (%) | PCE (Pt)/% | Ref. |
|---|---|---|---|---|---|---|
| $MoS_2$/RGO[a] | 12.51 | 0.73 | 0.66 | 6.04 | 6.38 | S5 |
| $NiS_2$/RGO[a] | 16.55 | 0.75 | 0.69 | 8.55 | 8.15 | S6 |
| CNT@$CoS_{1.097}$[a] | 14.26 | 0.77 | 0.66 | 7.18 | 7.11 | S7 |
| NGr/$MoS_2$[a] | 15.36 | 0.77 | 0.66 | 8.25 | 7.82 | S8 |
| CoS-GQDs[a] | 13.83 | 0.78 | 0.68 | 7.30 | 6.94 | S9 |
| $Co_9S_8$/rGO[a] | 15.24 | 0.70 | 0.66 | 7.10 | 7.45 | S10 |
| $MoS_2$/CNTs[a] | 16.65 | 0.74 | 0.66 | 7.83 | 7.15 | S11 |
| $MoS_2$/GA[a] | 17.24 | 0.71 | 0.64 | 7.86 | 7.23 | S12 |
| CNTs/$VS_2$[a] | 15.57 | 0.76 | 0.68 | 8.02 | 6.49 | S13 |
| $CoS_{1.097}$/RGO[a] | 14.85 | 0.70 | 0.66 | 6.85 | 7.14 | S14 |
| $CuMnSnS_4$/CNTs[a] | 16.53 | 0.72 | 0.72 | 8.97 | 8.37 | S15 |
| **NiS/CNTs** | **22.87** | **0.72** | **0.65** | **10.82** | **8.03** | **This work** |

[a] RGO is reduced graphene oxide, CNTs is carbon nanotube, NGr is nitrogen-doped graphene, GQDs is graphene quantum dots, GA is graphene aerogel.

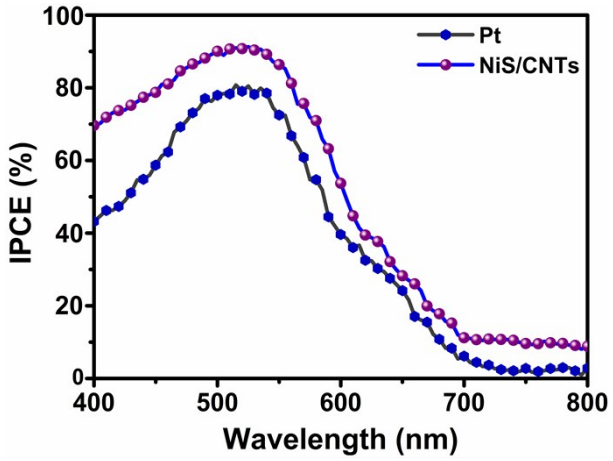


**Fig.S8** IPCE curves of the DSSCs with Pt and NiS/CNTs CEs.

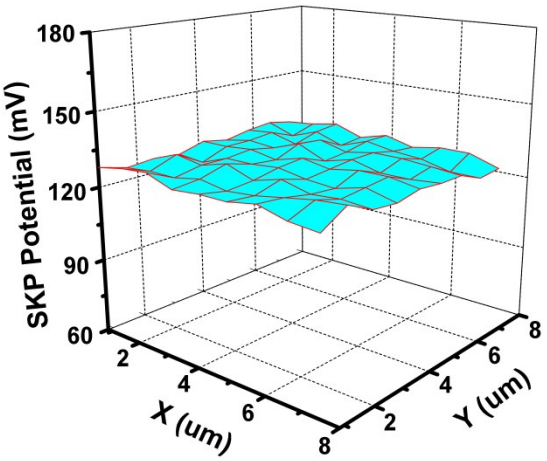


**Fig. S9** Work function map of NiS/CNTs-M.

**Table S3** The adsorption data of $I_3^-$ complex on the surface of NiS (101) and NiS/CNTs.

| Samples | $E_b$ (eV) | bond length[a] (Å) | |
|---|---|---|---|
| | | $I_1$-$I_2$ | $I_2$-$I_3$ |
| NiS (101) | -2.886 | 3.302 | 2.738 |
| NiS/CNTs | -1.364 | 3.171 | 2.791 |

[a] The bond length of free $I_1$-$I_2$ ($I_2$-$I_3$) and $I_2$ molecule is about 2.99, 2.70 Å, respectively.

## Additional references here:

S1. J. Clark Stewart, D. Segall Matthew, J. Pickard Chris, J. Hasnip Phil, I. J. Probert Matt, K. Refson and C. Payne Mike, *Z. Krist-Cryst. Mater.,* 2005, **220**, 567-570.

S2. J. P. Perdew, K. Burke and M. Ernzerhof, *Phys. Rev. Lett.*, 1996, **77**, 3865-3868.

S3. H. J. Monkhorst and J. D. Pack, *Phys. Rev. B*, 1976, **13**, 5188-5192.

S4. B. G. Pfrommer, M. Côté, S. G. Louie and M. L. Cohen, *J. Comput. Phys.*, 1997, **131**, 233-240.

S5. C.-J. Liu, S.-Y. Tai, S.-W. Chou, Y.-C. Yu, K.-D. Chang, S. Wang, F. S.-S. Chien, J.-Y. Lin and T.-W. Lin, *J. Mater. Chem.*, 2012, **22**, 21057-21064.

S6. Z. Li, F. Gong, G. Zhou and Z.-S. Wang, *J. Phys. Chem. C*, 2013, **117**, 6561-6566.

S7. J.-Y. Lin, S.-Y. Tai and S.-W. Chou, *J. Phys. Chem. C*, 2014, **118**, 823-830.

S8. M.-S. Fan, C.-P. Lee, C.-T. Li, Y.-J. Huang, R. Vittal and K.-C. Ho, *Electrochim. Acta*, 2016, **211**, 164-172.

S9. Y. Chang, L. Zhiqiang, C. Yiwen, M. Xiangtong, L. Mingyu and Q. Jieshan, *Sci. China Mater.*, 2016, **59**, 104.

S10. H. Yuan, Q. Jiao, J. Liu, X. Liu, H. Yang, Y. Zhao, Q. Wu, D. Shi and H. Li, *J. Power Sources*, 2016, **336**, 132-142.

S11. C.-H. Lin, C.-H. Tsai, F.-G. Tseng, C.-C. M. Ma, H.-C. Wu and C.-K. Hsieh, *J. Alloy. Compd.*, 2017, **692**, 941-949.

S12. J. Ma, W. Shen and F. Yu, *J. Power Sources*, 2017, **351**, 58-66.

S13. G. Yue, X. Liu, Y. Mao, H. Zheng and W. Zhang, *Mater. Today Energy*, 2017, **4**, 58-65.

S14. H. Yuan, J. Liu, H. Li, K. Su, X. Liu, Y. Li, D. Shi, Q. Wu, Y. Zhao and Q. Jiao, *Carbon*, 2018, **126**, 514-521.

S15. X. Liu, L. Gao, G. Yue, H. Zheng and W. Zhang, *Solar Energy*, 2017, **158**, 952-959.